Recent Developments of the Arbitrary Lagrangian-Eulerian Containment Code ALICE-II

C.Y. Wang, W.R. Zeuch

Reactor Analysis and Safety Division, Argonne National Laboratory, 9700 South Cass Avenue, Argonne, Illinois 60439, U.S.A.

As discussed at SMiRT-5 (Berlin, 1979) the ANL arbitrary Lagrangian Eulerian containment code ALICE was developed for use in fast reactor containment studies and is particularly suited for problems involving complex fluid-structure interactions. Since then many improvements have been made which has resulted in a second version of the code, ALICE-II. A selection of some important improvements are given in this paper.

To realistically analyze the above-core hydrodynamics containing a movable upper internal structure (UIS), a 3-D pipe element has been adopted to calculate the response of the UIS columns that connect the UIS to the vessel head. A corotational coordinate scheme for large displacement, small strain, elastic-plastic structural-dynamic analysis is utilized in the formulation. Both geometric and material nonlinearities are considered. The governing equations are integrated explicitly using a central difference procedure.

Regarding the hydrodynamics and fluid-structure couplings, the extensive use of ALICE-II has highlighted, continuously, many code extensions and improvements. Briefly, capabilities have been introduced to treat the curved reactor bottom simulated by highly irregular cells, sliding conditions at the internal thin shells or skirts, flow through perforated structures, free-surface boundary conditions associated with large amplitude fluid-boundary motion, and the effect of sharp corners of various internals on the volume computation of the greatly distorted core-gas bubble.

In connection with the work on sodium fires, the sodium spillage model also has been augmented in which both the position and orientation of the penetration opening can be made arbitrary to simulate various leak paths. The analytical model further accounts for losses due to friction and flow-area change to reduce the conservatism inherent in the analysis based on the inviscid boundary condition. Thus, the overall procedure of calculating sodium spillage is more rigorous and simpler than the conventional methods.

As a result of these recent developments, ALICE-II has become a state-of-the-art tool and a very powerful code, with more flexibility and efficiency than other comparable codes. For instance, using the ALICE-II code not only eliminates the mesh distortion problem associated with the purely Lagrangian technique, but also simplifies the scheme of treating fluid-structure interaction utilized by the purely Eulerian method. Moreover, since ALICE-II uses an Eulerian free-surface algorithm, it has decisive advantages over the purely finite element method in treating a highly distorted core-gas bubble, as well as flow through perforated structures and sodium spillage.

1. Introduction

The development of the ANL arbitrary Lagrangian Eulerian code ALICE as a useful tool in containment analysis for fast reactor safety studies has been described at SMiRT-5 [1] held in Berlin, 1979. The salient features of the ALICE code at that time were the choice of Lagrangian, Eulerian, or hybrid Lagrangian Eulerian fluid mesh, the option of using the implicit or explicit time-integration scheme in the hydrodynamics, the implicit treatment of density variation in the fluid EOS, the Eulerian treatment of the fluid boundaries, as well as two-dimensional finite-element analysis of containment structures.

Since 1979 development of this code has continued by ANL not only in extending its calculational capabilities, but also in correcting shortcomings as detected by its wide applications and experimental validations. These improvements include treatments of: (1) the three-dimensional response of the support columns of the upper internal structure (UIS), (2) the irregular cell adjacent to the hemispherical reactor bottom and its associated fluid-structure interaction, (3) sliding conditions at the internal thin shells or skirts, (4) flow through perforated structures, (5) large amplitude free-surface motion, (6) greatly distorted core-gas bubble, and (7) sodium spillage. These developments and improvements have resulted in a second version of the code, ALICE-II [2,3].

In this paper, many selected ALICE-II capabilities are briefly described, including those for the 3-D UIS column response, the curved reactor bottom, flow through perforated structure, as well as bubble volume computation. Since schemes for treating the large amplitude free-surface motion and sodium spillage are quite similar to those of the ICECO-CEL code, they are omitted here but are given in Ref. [4].

2. Three-dimensional Structural Analysis

A three-dimensional general purpose pipe element, which was developed by Moneim, Chang, and Belytschko for the piping-response code SHAPS [5] using a corotational coordinate formulation [6], was used to model the response of the UIS support columns subjected to the upward force transmitted from the assembly portion of the UIS. Each element has eight degrees of freedom per node. Six degrees of freedom, three displacements and three rotations, describe the flexural motion in three-dimensional space. The remaining two degrees of freedom describe the axisymmetric breathing mode in terms of hoop displacement and wall bending rotation generated by the pressure wave transmitted from the fluid inside the pipe. Figure 1 shows a generic pipe element. A detailed formulation of this element is given in Ref. [5].

In the co-rotational coordinates finite element formulation, the application of the equations of motion is shown to be equivalent to the direct application of Newton's second law to each node. For the pipe element, the translational equations of motion are separated from the moment and rotational equations. The translational equations are written in the fixed global coordinate system, whereas the moment and rotational equations are written in the nodal body coordinate system. The purpose of this separation is simplicity of equations and efficiency of computations.

The simplicity of the moment equations is achieved because the nodal body coordinate system is, by definition, the principal axis of the nodal mass. Thus, the moment equations are actually the Eulerian equations of motion. The efficiency of computations is realized because the moment of inertia tensor remains unchanged with time since the nodal body coordinate system rotates with the node, and thus remains aligned with the principal axes of the nodal mass. Therefore, the moment of inertia tensor is computed only once rather than computed at each node in every time cycle, as would be the case if the moment equations were written with respect to a fixed coordinate system.

The displacement field of the pipe element consists of cubic transverse displacements, linear axial and torsional displacements. Resultant forces are generally computed by three-point numerical integrations across the depth of the element, five-point integrations across the circumference, and two-point integrations along the length of the element.

3. Two-Dimensional Hydrodynamics

3.1 Hemispherical Reactor Bottom and Fluid-Structure Interaction

The region near the hemispherical reactor bottom is usually approximated by many highly irregular cells. A scheme has been developed to determine the radial and axial cell numbers associated with each particle in this region. This is necessary for determining cells which are full, partially full, or empty of fluid.

Figure 2 describes, schematically, the method used to assign individual marker particles to fluid zones. A preliminary zone is found by searching the r and z coordinates of the zone vertices and comparing these with the marker particle coordinates. When a likely zone is found, the vertices are numbered and the equations of the four lines containing the four segments in the r-z plane are determined. The marker particle coordinates are then compared to each of these equations to determine whether the particle is in the half space which is greater or less than each of these four lines. If the following conditions are satisfied:

$$\begin{aligned} z &\geq L_{12}\ (r) \\ r &< L_{23}\ (z) \\ z &< L_{34}\ (r) \\ r &\geq L_{41}\ (z) \end{aligned} \tag{1}$$

where r and z are the radial and axial marker particle coordinates, and L_{12}, L_{23}, L_{34}, L_{41} are the equations of the four lines forming the zone, then the marker particle is within the zone (see Fig. 2b). If the conditions are not met, sufficient information is known to move the search in the proper direction (see Fig. 2a). This method is applicable to very irregular zones and requires very few iterations.

The boundary conditions at the fluid-structure interface require that the fluid may slide freely along the structure surface, but must move together with the structure in the normal direction. Figure 3 shows the structural segments with nodal points 1, 2, and 3 located on the side of the fluid cells A and B with corresponding fluid nodes 1′, 2′, and 3′. We assume that the normal direction at point 2 is determined by the line connecting points 1 and 3. Thus, the boundary conditions, requiring that the fluid velocities to be changed from $u_{2'}$ and $v_{2'}$ to $u_{2'}'$ and $v_{2'}'$, are [7]

$$u_{2'}' = u_2 \sin^2\theta - v_2 \sin\theta \cos\theta + u_{2'} \cos^2\theta + v_{2'} \sin\theta \cos\theta \ , \tag{2}$$

and

$$v_{2'}' = - u_2 \sin\theta \cos\theta + v_2 \cos^2\theta + u_{2'} \sin\theta \cos\theta + v_{2'} \sin^2\theta \ , \tag{3}$$

where

$$\theta = \cos^{-1}\left[\frac{x_3 - x_1}{\sqrt{(x_3 - x_1)^2 + (y_3 - y_1)^2}}\right] , \tag{4}$$

and u_2 and v_2 are the radial and axial velocity components at structural nodal point 2.

Since the vertices of the fluid cell adjacent to the structure have been moved with different velocities from the structural nodal points, a rezone calculation is required in the third phase to compute the convective flux due to the relative motion between the fluid and the computing mesh as the fluid vertices move back to coincide with the structural nodal points.

3.2 Flow Through Perforated Structures

Analysis of flow through perforated structures is a difficult problem since it involves the treatment of the flow around sharp corners, which impose some problems for the ALICE code. The reason for this is that, in the ALICE analysis, the velocities are defined at the cell vertices. As can be seen from Fig. 4, the fluid velocity at the corner point 4 of cell A is discontinuous.

To solve the fluid-flow problem at a sharp corner, a scheme similar to that used in the ICECO code [4] has been adopted for calculation of the fluid motion. For instance, to calculate the fluid velocity between cells C and B at the corner point, cell A is treated as if it were occupied by a structure; to calculate the fluid velocity between cells B and A at the corner point, cell C is treated as if it were occupied by a structure. Thus, eqs. (2) and (3) can be used for the velocity calculations, except that the angle along the structural surface 64 becomes

$$\theta_{64} = \cos^{-1}\left[\frac{x_6 - x_4}{\sqrt{(x_6 - x_4)^2 + (y_6 - y_4)^2}}\right] , \tag{5}$$

and the angle along the structural surface 41 becomes

$$\theta_{41} = \cos^{-1}\left[\frac{x_4 - x_1}{\sqrt{(x_4 - x_1)^2 + (y_4 - y_1)^2}}\right] . \tag{6}$$

3.3 Highly Distorted Core-Gas Bubble and its Volume Integration

During an HCDA the core-gas bubble usually is severely distorted due to the presence of various internal structures adjacent to the core. In the ALICE code system the bubble-coolant interface is treated by a purely Eulerian method similar to that of the ICECO code [4]. Thus, correct boundary conditions can be rigorously applied near the bubble-coolant interface and large distortion of the core-gas bubble can be reasonably treated. However, in the original version of the ALICE code, the volume of the core-gas bubble is computed by means of marker particles without considering the effect of various internals even when the bubble is highly distorted. This volume calculation is an approximation which may introduce error in the source pressure computation for problems involving many internals.

To preserve the accuracy of the core-volume calculation a new scheme has been introduced into the ALICE-II code, in which fictitious marker particles representing corners of reactor internals are added sequentially into core particles to perform the volume integration. Figure 5 schematically shows a detail of the core-gas bubble expansion around an obstacle boundary. Figure 5a shows the marker particles moving with the fluid around the obstacle. A volume calculation using this marker particle configuration would introduce errors (indicated by the dotted line connecting particles 3 and 4 through the obstacle). To prevent this from occurring, the new volume algorithm flags the presence of obstacle zones between marker particles and performs calculations to determine whether or not the connecting segment passes through the obstacle. If this is the case, (as in Fig. 5a), a new, fictitious marker particle is inserted at the corner of the obstacle and the original particles are renumbered. Figure 5b shows, schematically, how this occurs. A new fictitious particle 4 is inserted at the corner of the obstacle and the former particles 4 and 5 are renumbered to 5 and 6.

4. Results

4.1 Effects of Perforated Plate on the Containment Response

The first problem deals with a study of the effects of a perforated plate on the slug impact load and containment response. The mathematical model used in the ALICE-II analysis is shown in Fig. 6. The reactor configuration consists of a primary vessel, a core barrel, a perforated dip plate, and a movable reactor cover with holddown bolts. Marker particles are used to represent coolant. Two calculations have been performed with the ALICE-II code: one with and the other without the perforated dip plate.

Figure 7 presents reactor configurations at three different times for the case with the perforated plate. These configurations show how the core-gas bubble expands and how the core barrel and primary vessel deform during the excursion. In addition, Fig. 7 indicates significant flow blockage near the bottom of the perforated plate.

Reactor configurations for the case without the perforated plate are shown in Fig. 8. By comparing the configurations for the two cases given in Figs. 7 and 8, it is evident that the perforated plate has the effect of (1) confining the HCDA bubble expansion, (2) slowing down the upward movement of the coolant slug, (3) changing the smooth coolant free surface to a relatively turbulent one, and (4) reducing the slug-impact loads and the upper vessel wall deformation. However, the increase in core barrel deformation owing to the slower core-gas bubble expansion, which results from the suppression effect of the perforated plate, is quite small.

From this study, it can be concluded that the perforated plate does play an important role in the overall containment response; in particular, it has a mitigating effect on the slug impact and upper vessel deformation.

4.2 Integrated Analysis of Containment Response and Sodium Spillage

The reactor configuration used in this study is shown in Fig. 9a. It consists of a reactor core, a primary vessel, and various internal components. One penetration hole is assumed to be located in the vessel head (shown by the dotted lines) to indicate the location of the leak path. This penetration is closed initially, but will open after being acted upon by a prescribed impulse. Marker particles are used to denote coolant. The initial core pressure was taken to be about 26.3 MPa.

Figure 9b-c shows reactor configurations at three different times. These configurations illustrate: (1) how the coolant disturbance occurs in the bottom portion of the reactor from pressure waves propagating downward through the opening of the CSS, (2) how the core-gas bubble expands and is distorted as it encounters the sharp corners of various internal structures, (3) how the UIS columns displace laterally, (4) how the UIS is displaced upward and how it interacts with the core-gas bubble, as well as with the surrounding fluid, (5) how the fluid moves and how the free surface impinges on the reactor cover, and (6) how the radial shield, core barrel and the primary vessel are deformed during the course of the excursion. These deformations can be seen from the movements of cell vertices adjacent to these structures.

Regarding the sodium spillage, marker particle configurations also show some interesting phenomena after the slug impact. In Fig. 9b the penetration no longer can sustain the impulse generated by the slug impact and suddenly opens. Figure 9c shows that large amounts of coolant have already spilled out from the top penetration and the side opening at the vessel-cover junction. The sodium spillage phenomenon is of primary importance for the analysis of sodium fires in the secondary containment.

5. Acknowledgments

The authors would like to express their gratitude to Drs. Y. W. Chang and S. H. Fistedis for their encouragement. This work was performed in the Engineering Mechanics Program of the Reactor Analysis and Safety Division of Argonne National Laboratory, under the auspices of the U.S. Department of Energy.

References

[1] CHU, H. Y., "ALICE - An Arbitrary Lagrangian-Eulerian Code for Analyzing FBR Containment Response to HCDA," Trans. 5th Intl. Conf. on Structural Mechanics in Reactor Technology, paper E 1/4, Berlin (August, 1979).

[2] WANG, C. Y., ZEUCH, W. R., "ALICE-II: An Arbitrary Lagrangian Eulerian Code for Containment Analysis with Complex Internals," Trans. Am. Nucl. Soc., Vol. 41, p. 364 (June, 1982).

[3] WANG, C. Y., ZEUCH, W. R., "A Multi-Dimensional Arbitrary Lagrangian-Eulerian Method for Dynamic Fluid-Structure Interaction," in Fluid-Transients and Fluid/Structure Interaction, 1982 ASME Special Publication PVP-64, Book H00221, pp. 289-316 (June, 1982).

[4] WANG, C. Y., "ICECO-CEL: A Coupled Eulerian-Lagrangian Code for Analyzing Primary System Response in Fast Reactors," ANL-81-9, Argonne National Laboratory (February, 1981).

[5] A-MONEIM, M. T., CHANG, Y. W., BELYTSCHKO, T. B., "Three-dimensional Response of Piping Systems to Internally Propagating Pressure Pulses," paper E 3/3, SMiRT-5, Berlin (August, 1979).

[6] BELYTSCHKO, T. B., et al., "Large Displacement, Transient Analysis of Space Frames," Intl. J. Num. Meth. Eng., Vol. 11, p. 65 (1977).

[7] HIRT, C. W., et al., "An Arbitrary Lagrangian Eulerian Computing Method for all Fluid Speeds," J. Comp. Phys., Vol. 14, p. 227 (1974).

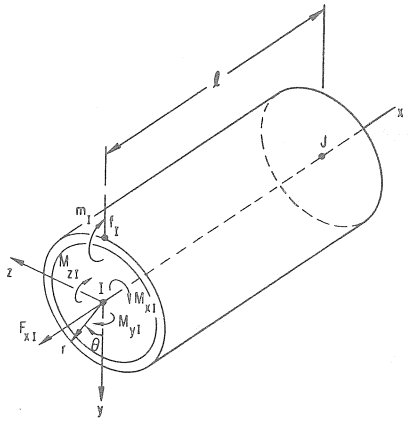

1. Generic Pipe Element

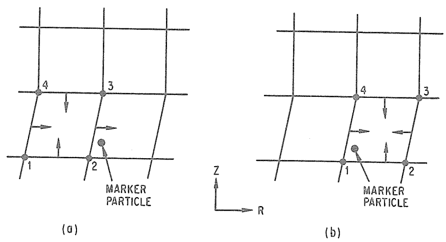

2. Determination of Computational Zone Associated with a Marker Particle

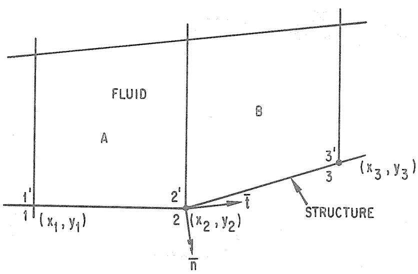

3. Fluid-Structure Coupling Calculation

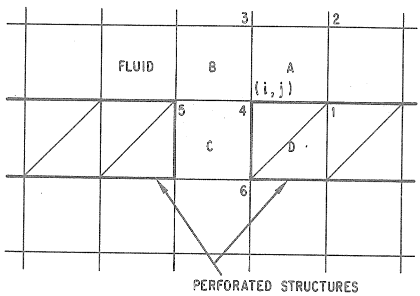

4. Fluid Flow at a Sharp Corner of the Perforated Structures

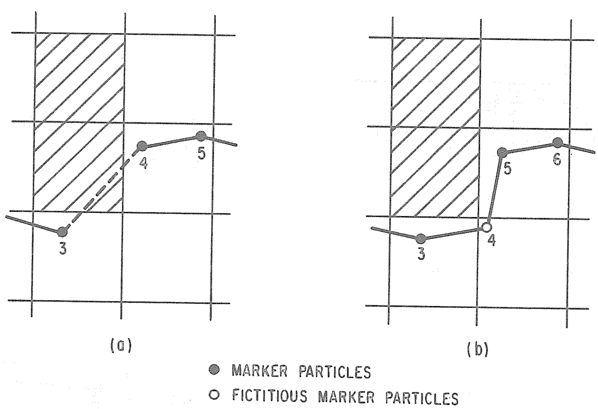

5. Detail of the Core-Gas Bubble Expansion

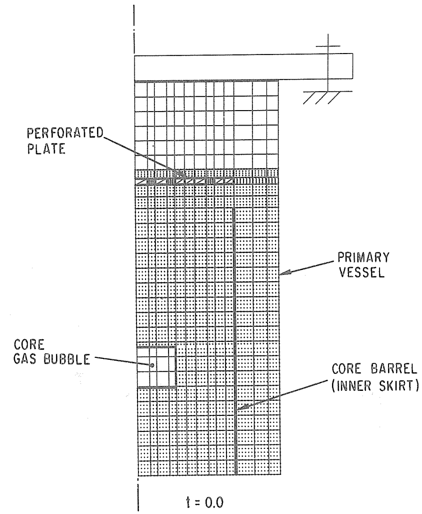

6. Initial Configuration Used in the ALICE-II Analysis

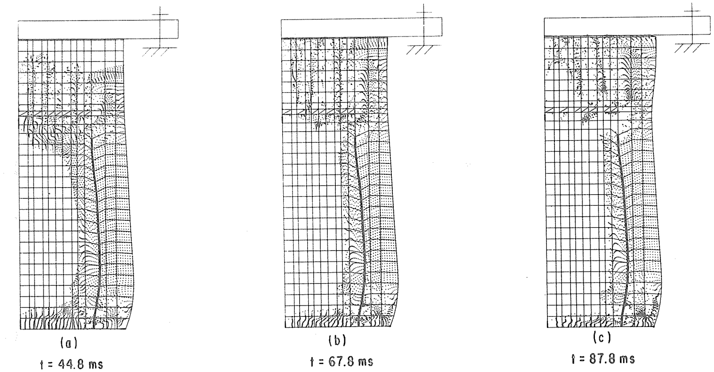

7. Reactor Configurations at Three Different Times: with the Perforated Plate

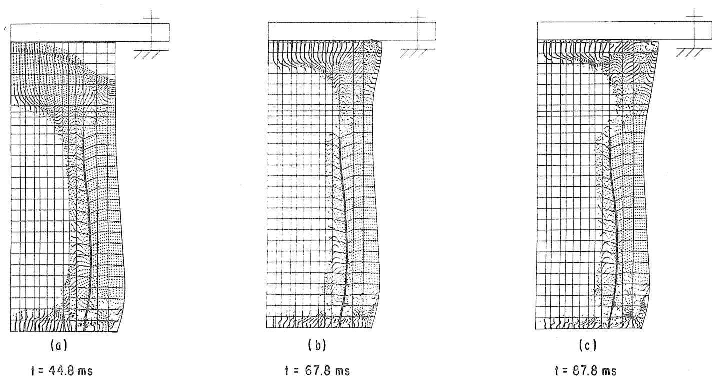

8. Reactor Configurations at Three Different Times: without the Perforated Plate

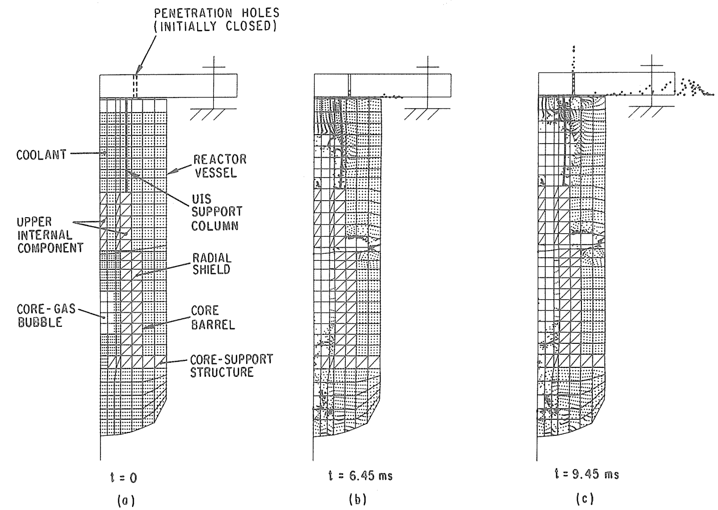

9. Reactor Configurations for Integrated Containment Analysis Involving Sodium Spillage